

Electronic Supplementary Information:

Singlet Exciton Fission in a Linear Tetracene Tetramer

*Heyuan Liu, Zhiwei Wang, Xuemin Wang, Li Shen, Chunfeng Zhang, Min Xiao, and Xiyu Li**

Content

1. The concentration-dependent absorption spectra of tetramer 4	2
2. Minimized molecular structure of tetramer 4	3
3. The normalized absorption spectra of compound 1-4 in toluene.....	4
4. The fluorescence dynamics of tetramer 4 in degassed toluene probed at different wavelengths	5
5. The temperature-dependent fluorescence property of tetramer	6
6. The transient absorption spectra of trimer 3	7
7. The sensitization experiment of tetramer 4	8
8. Comparison of TA spectra of tetramer 4 between the raw data and the fitting data	10
9. Comparison of the dynamics of trimer 3 and tetramer 4 probed at 416 nm and 490 nm.....	11
10. Comparison of triplet states obtained from iSF and sensitization	12
11. Fluence independent dynamics of tetramer 4	13
12. Solvent independent dynamics of tetramer 4.....	14
13. Singlet fission yield determination	15
14. The energy of the S ₁ , T ₁ and T ₂ states in tetracene.....	21
15. Copies of the ¹ H NMR spectra and MALDI-TOF spectra of new compounds	22
Reference.....	26

1. The concentration-dependent absorption spectra of tetramer 4

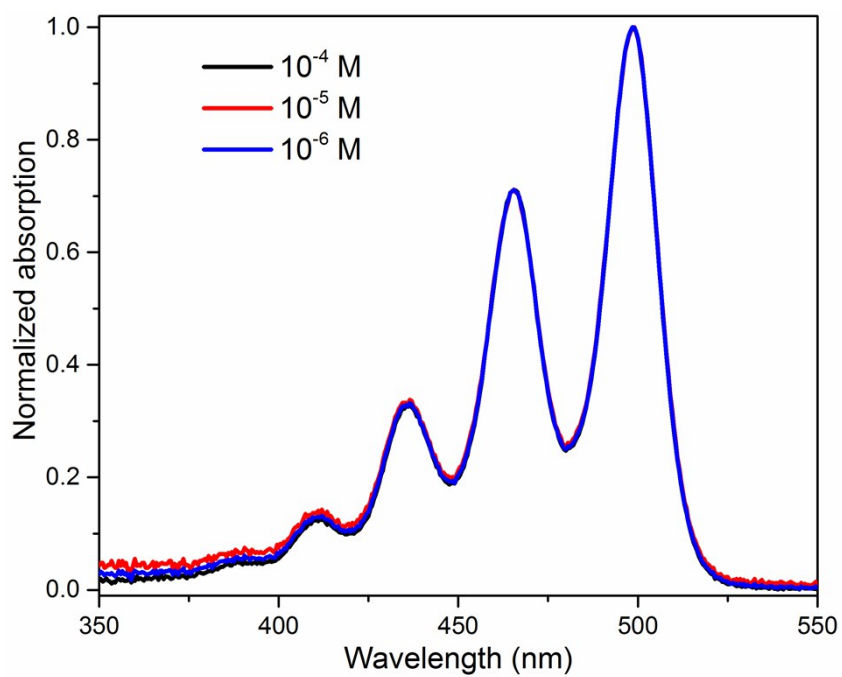


Fig. S1 The concentration-dependent absorption spectra of tetramer 4 in toluene.

2. Minimized molecular structure of tetramer 4

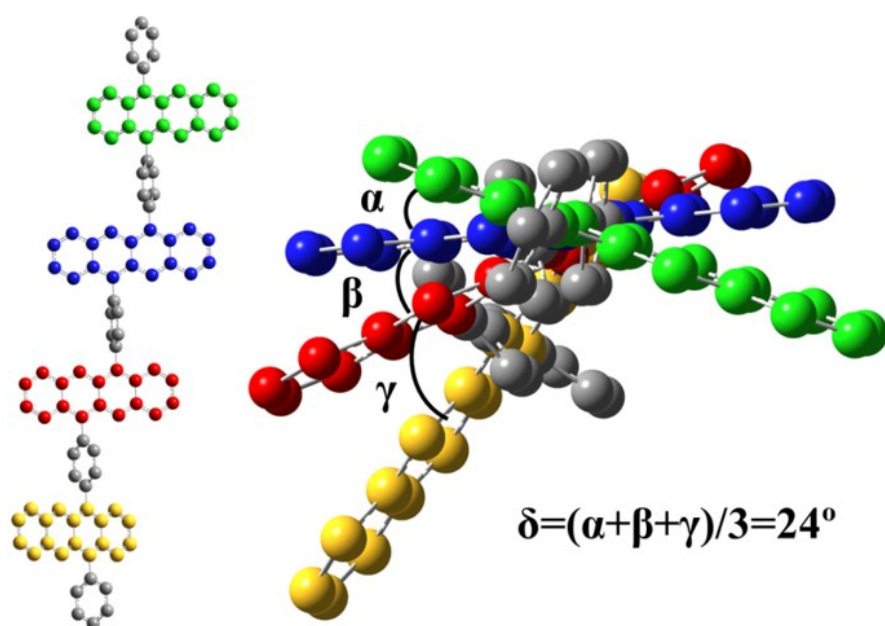


Fig. S2 The minimized molecular structure of tetramer 4. The calculated dihedral angle (24°) between the two neighboring tetracenes in tetramer 4 is smaller than those in trimer 3 (28°) and dimer 2 (32°).¹ The hydrogen atoms have been eliminated for the clarity. The calculations were performed at the B3LYP/6-31G*^{2,3} level of theory using the Gaussian 09 program⁴.

3. The normalized absorption spectra of compound 1-4 in toluene

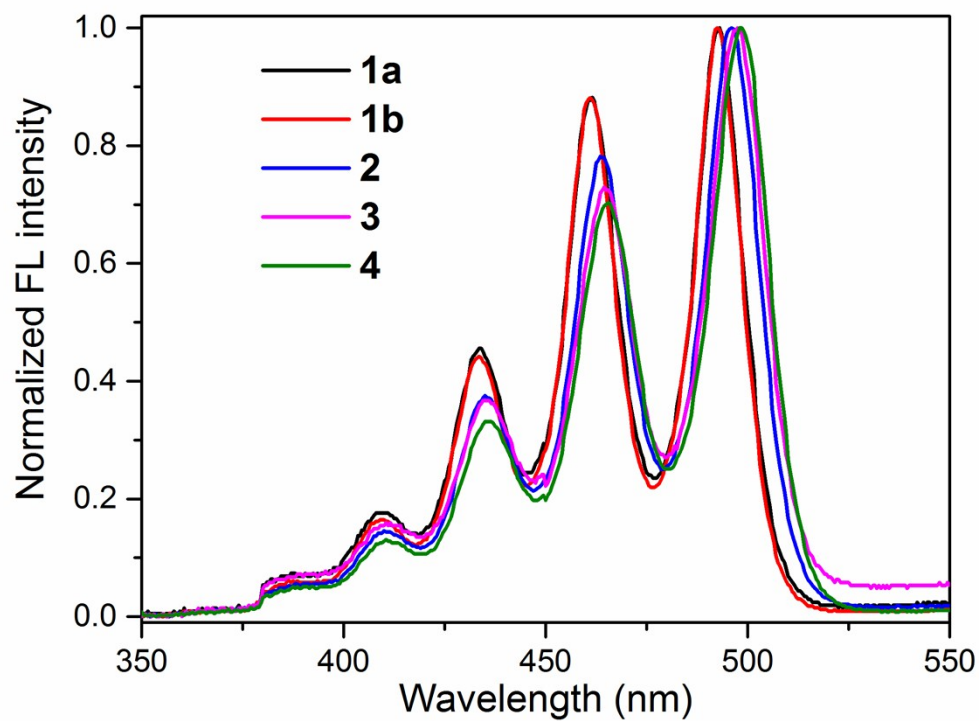


Fig. S3 The normalized absorption spectra of compound 1-4 in toluene.

4. The fluorescence dynamics of tetramer 4 in degassed toluene probed at different wavelengths

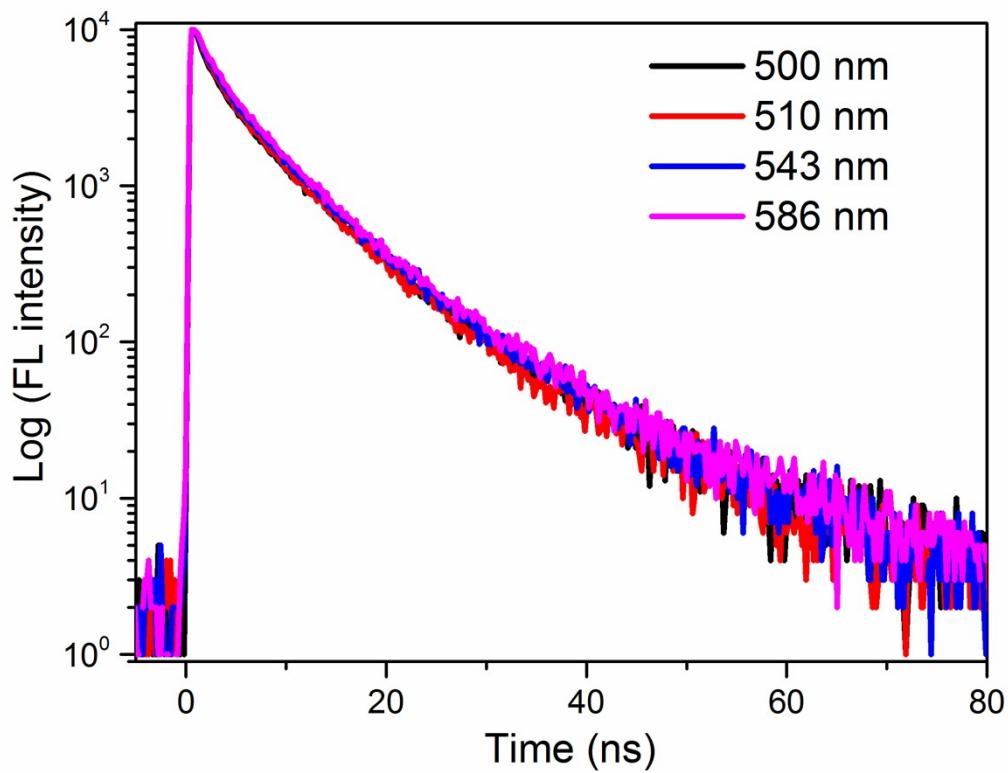


Fig. S4 The fluorescence dynamics of tetramer 4 in degassed toluene probed at different wavelengths (excited at 441 nm).

5. The temperature-dependent fluorescence spectra of tetramer

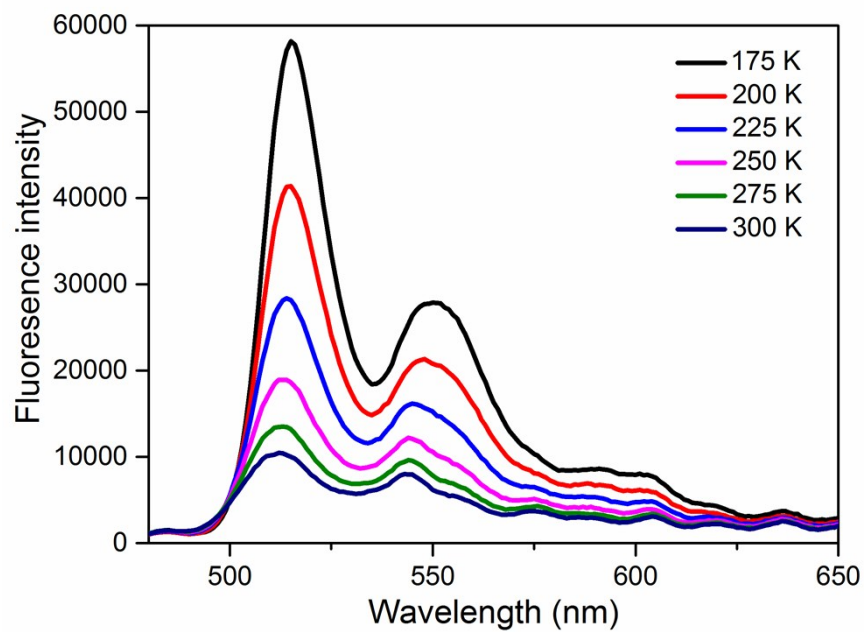


Fig. S5 The temperature-dependent fluorescence spectra of tetramer in degassed toluene (excited at 441 nm).

6. The transient absorption spectra of trimer 3

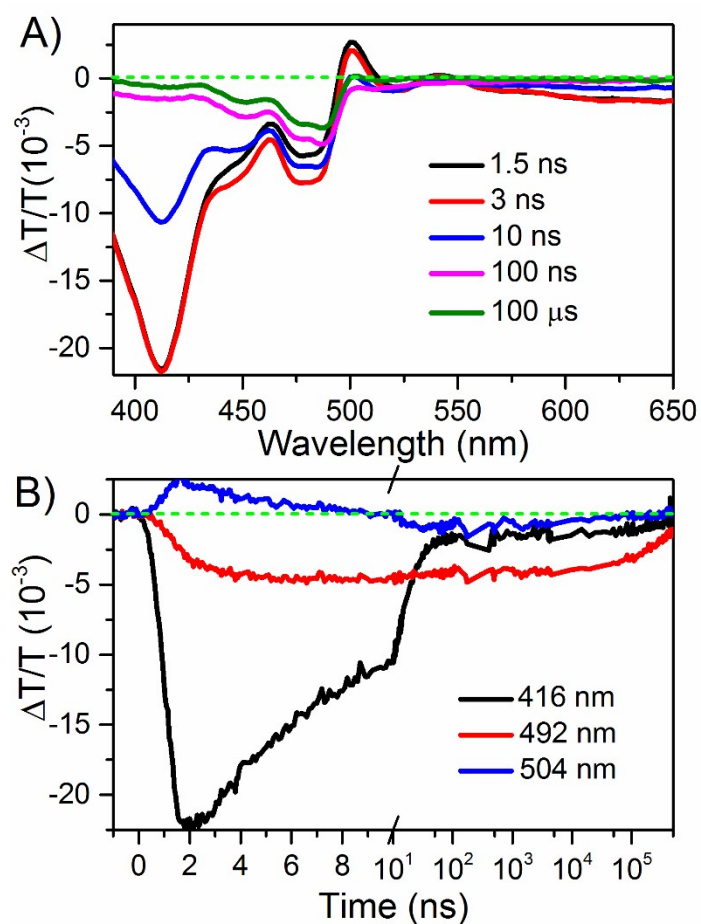


Fig. S6 (A) Nanosecond transient absorption spectra of trimer **3** in degassed toluene (excited at 355 nm). (B) The transient absorption dynamics of trimer **3** probed at different wavelengths.

7. The sensitization experiment of tetramer 4

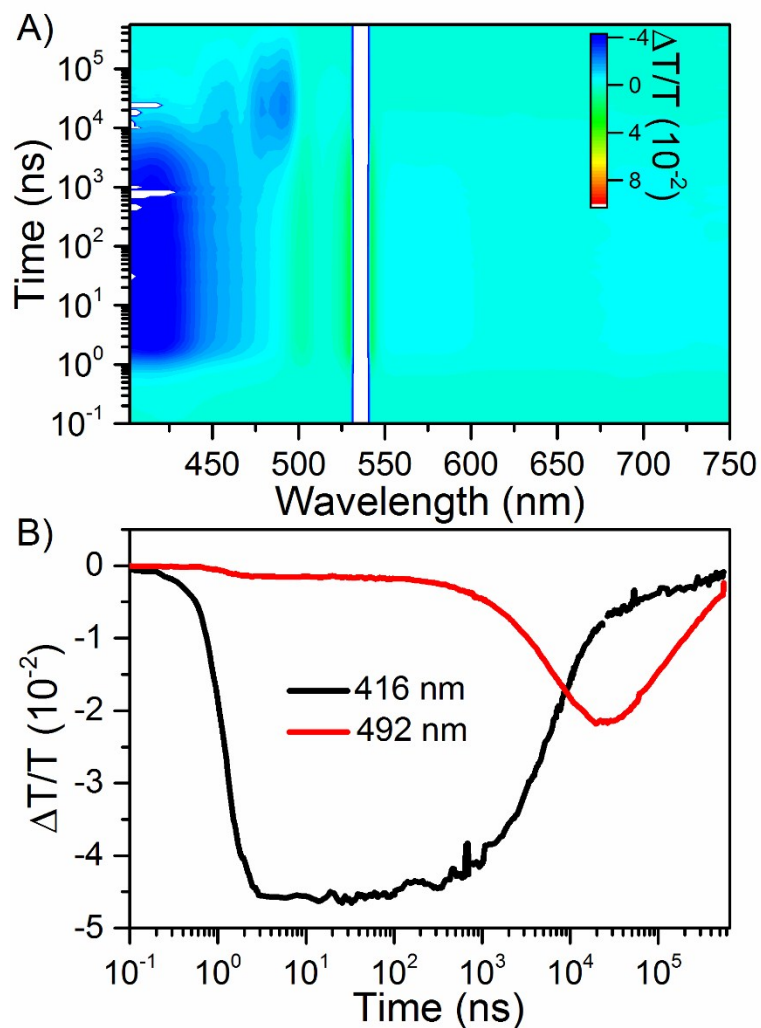


Fig. S7 A) Nanosecond TA measurements of PtOEP doped tetramer **4** in degassed toluene following excitation of PtOEP at 532 nm. B) The dynamics of tetramer **4** probed at different wavelengths.

To obtain the triplet spectral signature of tetramer **4** in solution, triplet sensitization of tetramer **4** in toluene was performed with a known triplet sensitizer, platinum octaethylporphyrin (PtOEP). Because the sensitization process is diffusion limited in solution, nanosecond TA measurements were performed following excitation of PtOEP at 532 nm of a PtOEP doped tetramer **4** solution (Figure S7). At initial times (1 ns-2 μ s), the only spectral signature observed corresponds to the reported T_1 - T_n absorption

(416 nm) of PtOEP (Figure S7A). As the time evolve, the triplet absorption of PtOEP at 416 nm decreases with a concomitant rise in a new induced absorption feature at about 492 nm (Figure S7B). This band is assigned to T_1 state of tetramer **4** based on its spectral similarity to that reported for T_1 - T_n absorption for trimer **3** and diphenyltetracene film.^{1,5}

8. Comparison of TA spectra of tetramer 4 between the raw data and the fitting data

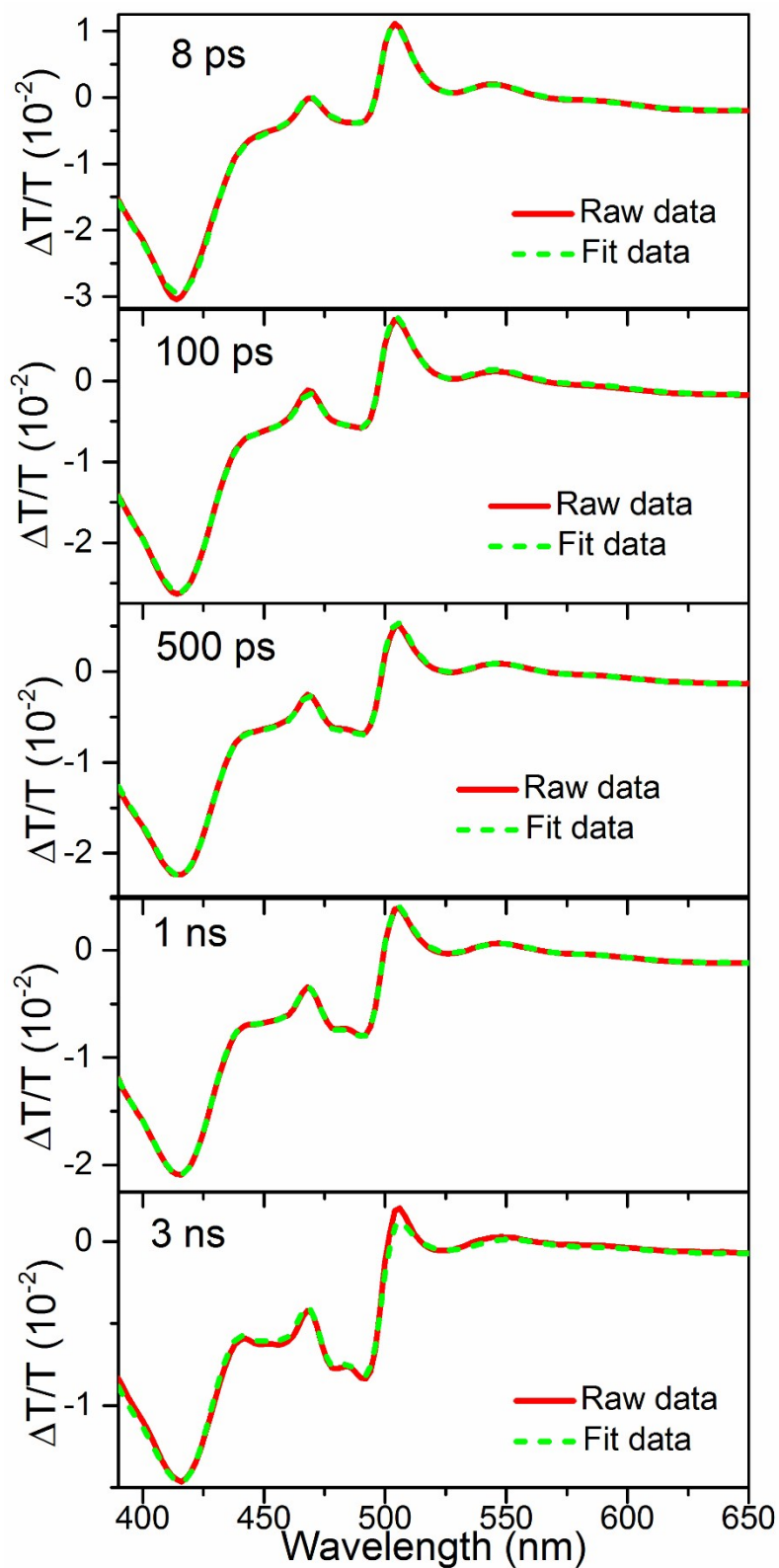


Fig. S8 Comparison of TA spectra of tetramer 4 between the raw data and the fitting data obtained from the SVD method.

9. Comparison of the dynamics of trimer 3 and tetramer 4 probed at 416 nm and 490 nm

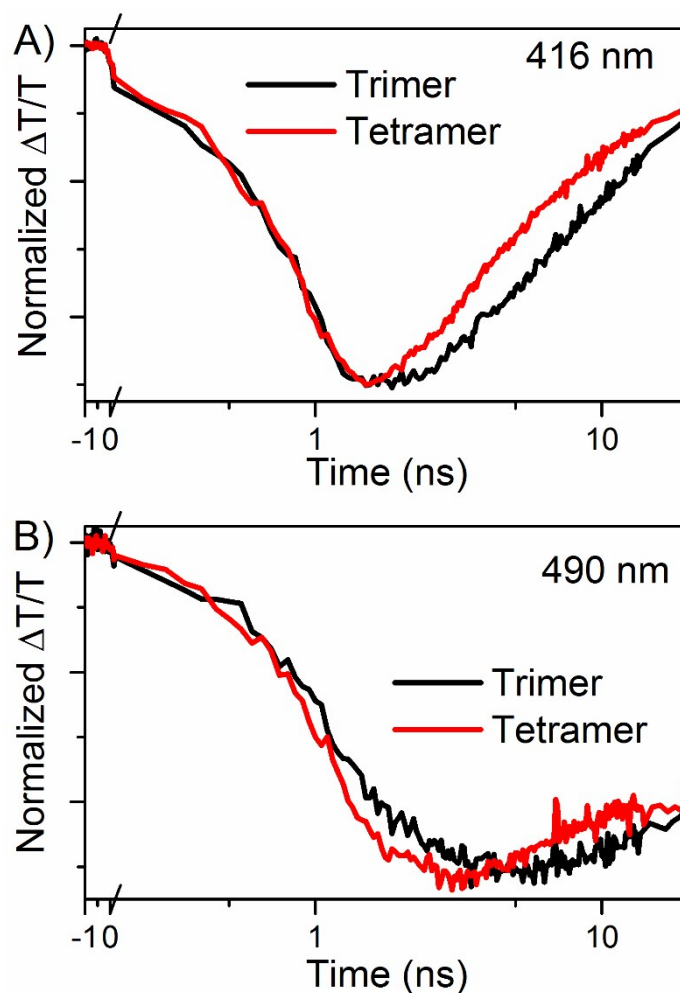


Fig. S9 The comparison of the dynamics of trimer 3 and tetramer 4 probed at 416 nm (A) and 490 nm (B) in degassed toluene.

10. Comparison of triplet states obtained from iSF and sensitization

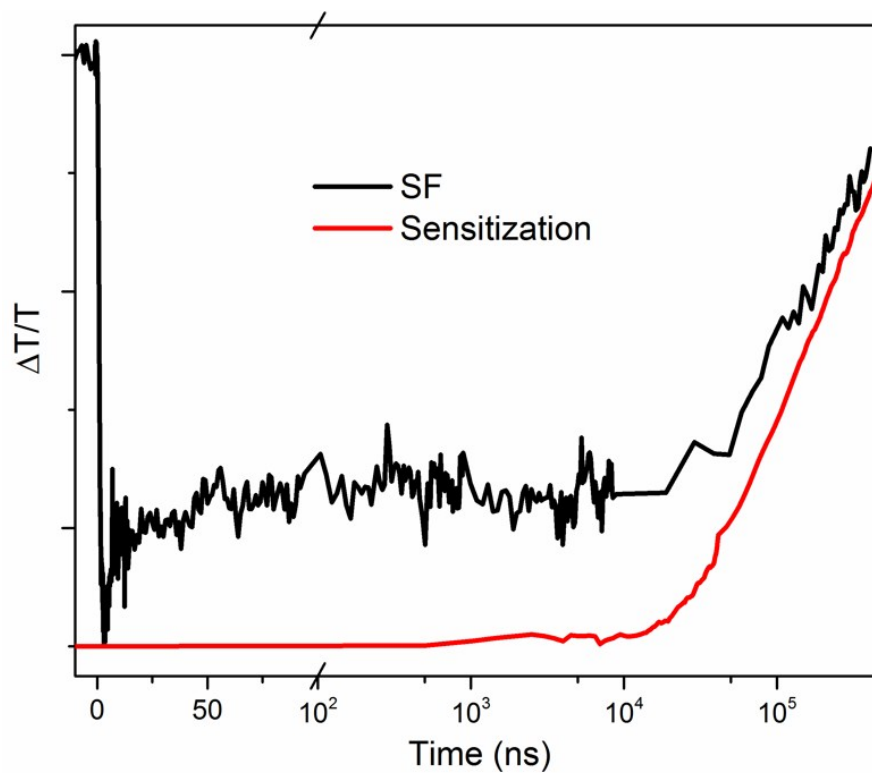


Fig. S10 Comparison of lifetimes of triplet states of tetramer **4** obtained from iSF and sensitization experiment. Sensitization data was offset along the x axis so that the maximum signal occurs at time zero according to the previous report.⁶

11. Fluence independent dynamics of tetramer 4

All dynamical behavior is independent of excitation fluence within the measured range (up to $200 \mu\text{J}/\text{cm}^2$). Single-wavelength kinetics at 416 nm and 492 nm are shown in Figure S11 as a function of the 493 nm pump fluence.

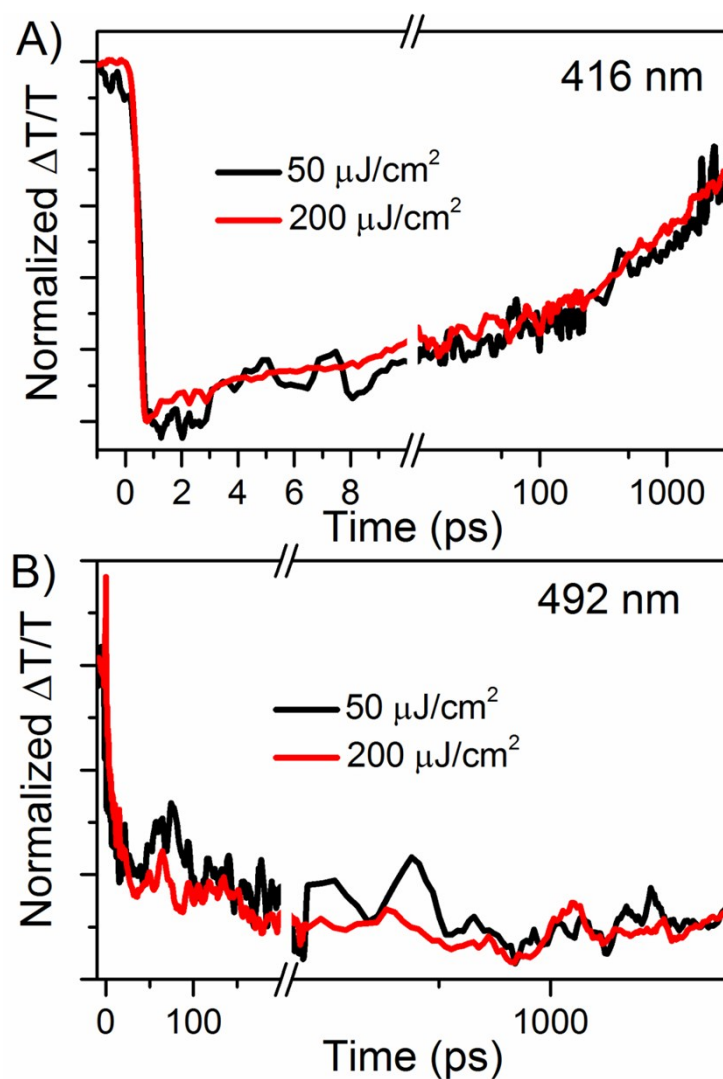


Fig. S11 Comparison of normalized dynamics of the absorption at 416 nm (A) and 492 nm (B), excited with 493 nm pump with varying pump fluence in degassed toluene.

12. Solvent independent dynamics of tetramer 4

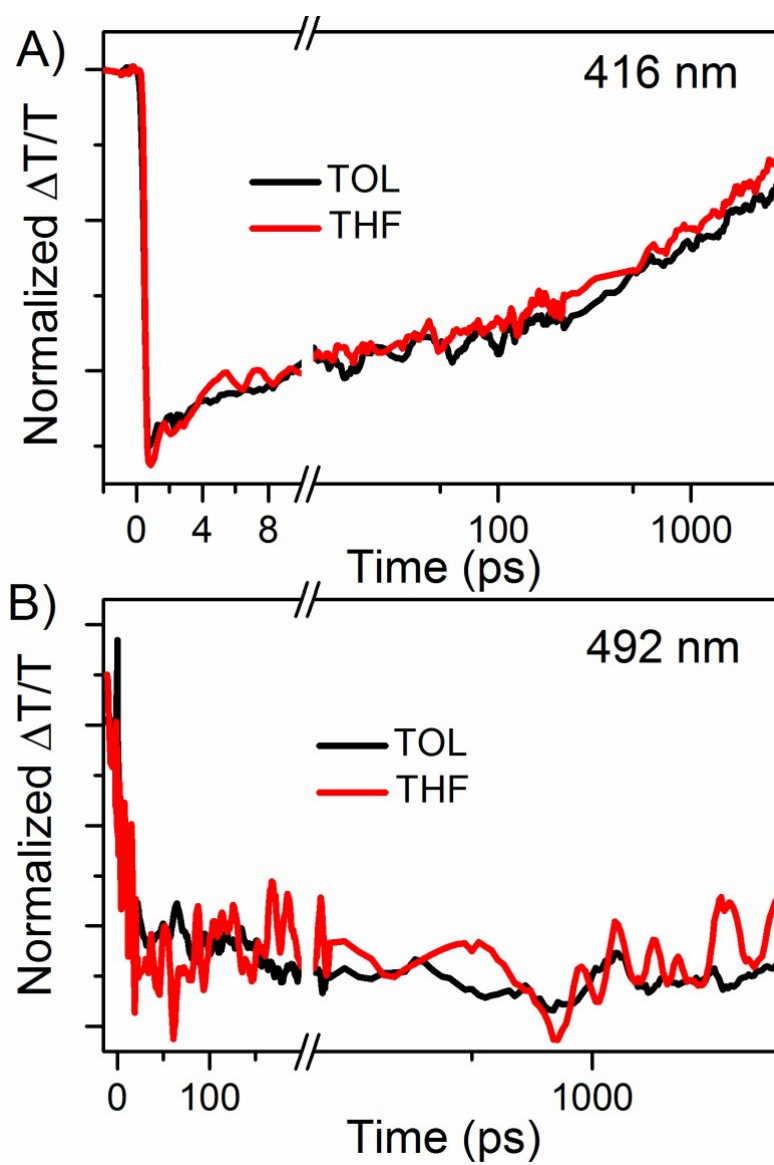


Fig. S12 The dynamics of tetramer 4 in different solvents probed at 416 (A) and 492 nm (B).

13. Singlet fission yield determination

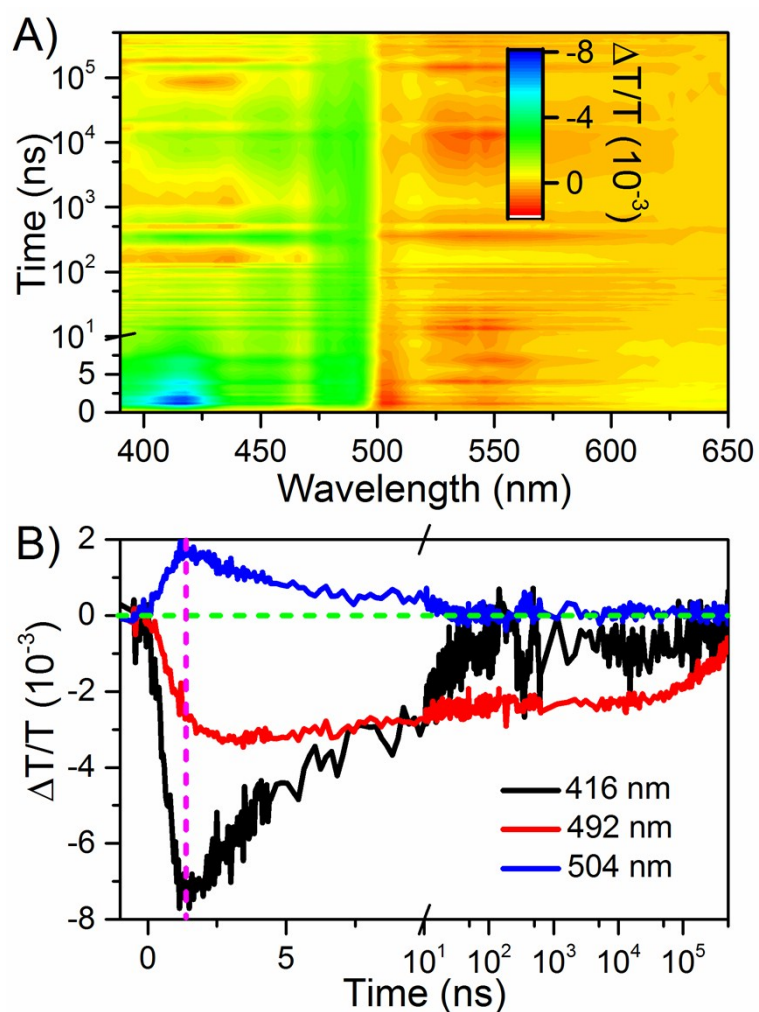


Fig. S13 Raw transient absorption data for tetramer **4** solution (7.2×10^{-5} M) with 355 nm excitation in degassed toluene.

In tetramer **4**, the similarity of the triplet state spectra obtained from sensitized experiment and iSF allowed us to determine the extinction coefficient of the triplet state of tetramer **4** from the sensitized experiment. Then, the concentration of the triplet state can be directly calculated from TA spectroscopy (100 ns) by using the Lambert-Beer law. The concentration of the singlet state can be calculated from the power of the

excitation light. At last, the triplet state quantum yield can be calculated by comparing the concentration of the triplet state with that of the singlet state.

The determination of the yield of triplet involves triplet sensitization experiments using a solution consisting of PtOEP and tetramer **4** excited at 532 nm. Triplets are generated in PtOEP by intersystem crossing and are then transferred to tetramer via collisional energy transfer.

A solution consisting of PtOEP (1.0×10^{-4} M) and tetramer **4** (5.1×10^{-5} M):

The total number of photons per pump pulse (532 nm):

$$\frac{\text{photons}}{\text{pulse}} = \frac{\text{power}}{(\text{rep rate})(\text{energy per photon})} = \frac{0.30 \times 10^{-3} \text{ W}}{500 \text{ s}^{-1} (3.73 \times 10^{-19} \text{ J photon}^{-1})} = 1$$

Spot volume (V):

$$V = \text{Area} \times d = \pi(350 \times 10^{-4} \text{ cm})^2 \times 0.2 \text{ cm} \times 0.001 \text{ L cm}^{-3} = 7.69 \times 10^{-7} \text{ L}$$

The fraction of light intensity transmitted (I/I_0) of PtOEP at 532 nm can be calculated as:

$$I/I_0 = 10^{-\epsilon_{532 \text{ nm}} c_{\text{PtOEP}} L} = 10^{-39500 \text{ cm}^{-1} \text{ mol}^{-1} \text{ L} \times 1 \times 10^{-4} \text{ mol L}^{-1} \times 0.2 \text{ cm}} = 0.16$$

The concentration of triplet exciton for PtOEP (c_T^{PtOEP}):

$$c_T^{\text{PtOEP}} = \frac{(\text{photons/pulse})(1 - I/I_0)}{N_A V} = \frac{(1.60 \times 10^{12}) \times 0.84}{(6.02 \times 10^{23} \text{ mol}^{-1})(7.69 \times 10^{-7} \text{ L})} = 2.90 \times 10^{-6} \text{ mol L}^{-1}$$

Triplet energy transfer efficient (Φ) was calculated by the ratio of the trimer triplet rise rate over the sum of the triplet rise rate and the PtOEP triplet decay rate:

$$\Phi = \frac{1/(8.50 \mu\text{s})}{1/(8.50 \mu\text{s}) + 1/(40 \mu\text{s})} = 82 \%$$

The concentration of triplet exciton for tetramer **4** obtained from PtOEP (c_T^{trimer}):

$$c_T^{trimer} = 2.90 \times 10^{-6} \text{ mol L}^{-1} \times 0.82 = 2.38 \times 10^{-6} \text{ mol L}^{-1}$$

In the nanosecond TA measurements of PtOEP doped tetramer **4**, the ESA signal of 492 nm at 30 μ s that the triplet energy transfer has completed (Figure S7B) is about -0.022. Therefore, the molar extinction coefficients of triplet absorption at 492 nm for tetramer **5** can be calculated as:

$$\epsilon_T^{492 \text{ nm}} = \frac{-\log_{10}(\Delta T/T + 1)}{c_T^{trimer} L} = \frac{-\log_{10}(-0.022 + 1)}{2.38 \times 10^{-6} \text{ mol L}^{-1} \times 0.2} = 2.02 \times 10^4 \text{ cm}^{-1} \text{ mol}^{-1} \text{ L}$$

In the ns-TA experiment of tetramer **4** (7.2×10^{-5} M), the ESA signal of 492 nm at 100 ns that the transient absorption spectrum is identical to that of the individual triplet state obtained from the sensitization experiment is about -0.0023. Using the calculated

$\epsilon_T^{492 \text{ nm}}$ from the sensitization experiment, the triplet concentration from SF can be calculated as:

$$c_T = \frac{-\log_{10}(\Delta T/T + 1)}{\epsilon_T^{492 \text{ nm}} L} = \frac{-\log_{10}(-0.0023 + 1)}{2.02 \times 10^4 \text{ cm}^{-1} \text{ mol}^{-1} \text{ L} \times 0.2 \text{ cm}} = 2.48 \times 10^{-7} \text{ mol L}^{-1}$$

Next, we calculated the concentration of the singlet state (c_S) by estimating the size of the initial ground state bleach amplitude based on the molar extinction coefficient.

Calculation at 504 nm:

$$c_S = \frac{\log_{10}\left(\frac{\Delta T}{T} + 1\right)}{\epsilon_{504 \text{ nm}} L} = \frac{\log_{10}(0.0018 + 1)}{3.8 \times 10^4 \times 0.2} = 1.03 \times 10^{-7} \text{ mol L}^{-1}$$

$$\Phi_{triplet} = \frac{c_T}{c_S} = \frac{2.48 \times 10^{-7} \text{ mol L}^{-1}}{1.03 \times 10^{-7} \text{ mol L}^{-1}} = 241\%$$

The triplet yield determined at this wavelength exceeds 200%, which is most likely due to the spectral overlap between the ESA and the bleach. This overlap can reduce

the amplitude of the ground state bleach so that the concentration of the singlet state was underestimated. As a result, the triplet yield was overestimated.

Calculation at 510 nm:

$$C_S = \frac{\log\left(\frac{\Delta T}{T} + 1\right)}{\varepsilon_{510nm}L} = \frac{\log(0.001126 + 1)}{1.466 \times 10^4 \times 0.2} = 1.67 \times 10^{-7} \text{ mol L}^{-1}$$

$$\Phi_{triplet} = \frac{c_T}{c_S} = \frac{2.48 \times 10^{-7} \text{ mol L}^{-1}}{1.67 \times 10^{-7} \text{ mol L}^{-1}} = 148\%$$

Calculation at 515 nm:

$$C_S = \frac{\log\left(\frac{\Delta T}{T} + 1\right)}{\varepsilon_{515nm}L} = \frac{\log(4.38 \times 10^{-4} + 1)}{0.49 \times 10^4 \times 0.2} = 1.94 \times 10^{-7} \text{ mol L}^{-1}$$

$$\Phi_{triplet} = \frac{c_T}{c_S} = \frac{2.48 \times 10^{-7} \text{ mol L}^{-1}}{1.94 \times 10^{-7} \text{ mol L}^{-1}} = 128\%$$

However, the GSB at 510 nm and 515 nm contains a slight of stimulated emission. This will cause a bit overestimated singlet concentration. Then, the triplet yield will be underestimated.

Propagated error in triplet yield determination:

The error of the preparation of a solution of PtOEP:

$$\frac{\delta(c_{PtOEP})}{c_{PtOEP}} = \sqrt{\left(\frac{\delta(m)}{m}\right)^2 + \left(\frac{\delta(V)}{V}\right)^2} = \sqrt{\left(\frac{0.02mg}{0.73mg}\right)^2 + \left(\frac{0.2mL}{10mL}\right)^2} = 0.035$$

Errors in determining the molar extinction coefficient of PtOEP at 532 nm:

$$\frac{\delta(\varepsilon_{532nm})}{\varepsilon_{532nm}} = \sqrt{\left(\frac{\delta(\Delta A)}{\Delta A}\right)^2 + \left(\frac{\delta(b)}{b}\right)^2 + \left(\frac{\delta(c_{PtOEP})}{c_{PtOEP}}\right)^2} = \sqrt{\left(\frac{0.001}{0.4}\right)^2 + \left(\frac{0.001cm}{1cm}\right)^2 + (0.035)^2} = 0.035$$

The propagated error of the fraction of light intensity absorbed (I/I_0) of PtOEP at 532 nm:

$$\begin{aligned}\frac{\delta(I/I_0)}{I/I_0} &= \varepsilon_{532\text{ nm}} c_{\text{PtOEP}} L \ln(10) \sqrt{\left(\frac{\delta(\varepsilon_{532\text{ nm}})}{\varepsilon_{532\text{ nm}}}\right)^2 + \left(\frac{\delta(c_{\text{PtOEP}})}{c_{\text{PtOEP}}}\right)^2 + \left(\frac{\delta(d)}{d}\right)^2} \\ &= 39500\text{ cm}^{-1}\text{ mol}^{-1}\text{ L} \times 1 \times 10^{-4}\text{ mol L}^{-1} \times 0.2\text{ cm} \times \ln(10) \sqrt{(0.035)^2 + (0.035)^2} \\ &= 0.10\end{aligned}$$

The error of photons per pump pulse in the sensitization experiment:

$$\begin{aligned}\frac{\delta\left(\frac{\text{photons}}{\text{pulse}}\right)}{\frac{\text{photons}}{\text{pulse}}} &= \sqrt{\left(\frac{\delta P}{P}\right)^2 + \left(\frac{\delta(\text{rep rate})}{\text{rep rate}}\right)^2 + \left(\frac{\delta(\text{energy/photon})}{\text{energy/photon}}\right)^2} \\ &= \sqrt{\left(\frac{0.15 \times 10^{-4}\text{ W}}{0.30 \times 10^{-3}\text{ W}}\right)^2 + \left(\frac{0.5\text{ Hz}}{500\text{ Hz}}\right)^2 + \left(\frac{6.22 \times 10^{-22}\text{ J}}{3.73 \times 10^{-19}\text{ J}}\right)^2} = 0.05\end{aligned}$$

The error of spot volume in the sensitization experiment:

$$\begin{aligned}\frac{\delta(V)}{V} &= \sqrt{\left(\frac{\delta(\text{Area})}{\text{Area}}\right)^2 + \left(\frac{\delta d}{d}\right)^2} \\ &= \sqrt{\left(\frac{6.42 \times 10^{-6}\text{ cm}^2}{3.85 \times 10^{-3}\text{ cm}^2}\right)^2 + \left(\frac{0.006\text{ cm}}{0.2\text{ cm}}\right)^2} = 0.03\end{aligned}$$

The error in determining the concentration of triplet exciton for PtOEP (c_T^{PtOEP}):

$$\frac{\delta(c_T^{\text{PtOEP}})}{c_T^{\text{PtOEP}}} = \sqrt{\left(\frac{\delta\left(\frac{\text{photons}}{\text{pulse}}\right)}{\frac{\text{photons}}{\text{pulse}}}\right)^2 + \left(\frac{\delta(I/I_0)}{I/I_0}\right)^2 + \left(\frac{\delta(V)}{V}\right)^2} = \sqrt{(0.05)^2 + (0.10)^2 + (0.03)^2} = 0.11$$

The propagated error of the molar extinction coefficients of the triplet absorption at 492 nm for tetramer **4** in the sensitization experiment:

$$\frac{\delta(\varepsilon_T^{492\text{ nm}})}{\varepsilon_T^{492\text{ nm}}} = \sqrt{\left(\frac{\delta(\Delta A)}{\Delta A}\right)^2 + \left(\frac{\delta(c_T^{\text{tetramer}})}{c_T^{\text{tetramer}}}\right)^2 + \left(\frac{\delta d}{d}\right)^2} = \sqrt{\left(\frac{4.0 \times 10^{-5}}{9.66 \times 10^{-3}}\right)^2 + (0.11)^2 + (0.03)^2} = 0.11$$

The propagated error of the triplet concentration from iSF in ns-TA of tetramer **4**:

$$\frac{\delta(c_T)}{c_T} = \sqrt{\left(\frac{\delta(\Delta A_{492\text{ nm}})}{\Delta A_{492\text{ nm}}}\right)^2 + \left(\frac{\delta(\varepsilon_T^{492\text{ nm}})}{\varepsilon_T^{492\text{ nm}}}\right)^2 + \left(\frac{\delta d}{d}\right)^2} = \sqrt{\left(\frac{0.4 \times 10^{-5}}{1 \times 10^{-3}}\right)^2 + (0.11)^2 + (0.03)^2} = 0.11$$

The error of the preparation of a solution of tetramer **4**:

$$\frac{\delta(c_{\text{tetracene}})}{c_{\text{tetracene}}} = \sqrt{\left(\frac{\delta(m)}{m}\right)^2 + \left(\frac{\delta(V)}{V}\right)^2} = \sqrt{\left(\frac{0.02\text{ mg}}{1.29\text{ mg}}\right)^2 + \left(\frac{0.2\text{ mL}}{10\text{ mL}}\right)^2} = 0.025$$

Errors in determining the molar extinction coefficient of tetramer at 510 nm:

$$\frac{\delta(\varepsilon_{510 \text{ nm}})}{\varepsilon_{510 \text{ nm}}} = \sqrt{\left(\frac{\delta(\Delta A)}{\Delta A}\right)^2 + \left(\frac{\delta(b)}{b}\right)^2 + \left(\frac{\delta(c_{PtOEP})}{c_{PtOEP}}\right)^2} = \sqrt{\left(\frac{0.001}{0.15}\right)^2 + \left(\frac{0.001 \text{ cm}}{1 \text{ cm}}\right)^2 + (0.025)^2} = 0.025$$

The propagated error of the singlet concentration from iSF in ns-TA of tetramer **4**:

$$\frac{\delta(c_s)}{c_s} = \sqrt{\left(\frac{\delta(\Delta A_{510 \text{ nm}})}{\Delta A_{510 \text{ nm}}}\right)^2 + \left(\frac{\delta(\varepsilon_{510 \text{ nm}})}{\varepsilon_{510 \text{ nm}}}\right)^2 + \left(\frac{\delta(d)}{d}\right)^2} = \sqrt{\left(\frac{0.4 \times 10^{-5}}{4.9 \times 10^{-4}}\right)^2 + (0.025)^2 + (0.03)^2} = 0.04$$

The propagated error of triplet yield of tetramer **4** (\square_{triplet}):

$$\begin{aligned} \frac{\delta(\square_{\text{triplet}})}{\square_{\text{triplet}}} &= \sqrt{\left(\frac{\delta(c_s)}{c_s}\right)^2 + \left(\frac{\delta(c_T)}{c_T}\right)^2} \\ &= \sqrt{0.04^2 + 0.11^2} = 0.12 \end{aligned}$$

14. The energy of the S₁, T₁ and T₂ states in tetracene

Table S1. The energy of the S₁, T₁ and T₂ states in tetracene

	S ₁ (eV)	T ₁ (eV)	T ₂ (eV)
Tetracene	2.322	1.201	2.568

The geometries and energies of the ground-state (S₀) and the first triplet state (T₁) were optimized with the DFT method. The optimization of excited state energies for S₁ and T₂ states were calculated using the time-dependent density functional theory (TDDFT) method based on the optimized S₀ and T₁ geometries, respectively. All the calculations were performed at the B3LYP/6-31G*^{2, 3} level of theory using the Gaussian 09 program⁴.

15. Copies of the ^1H NMR spectra and MALDI-TOF spectra of new compounds

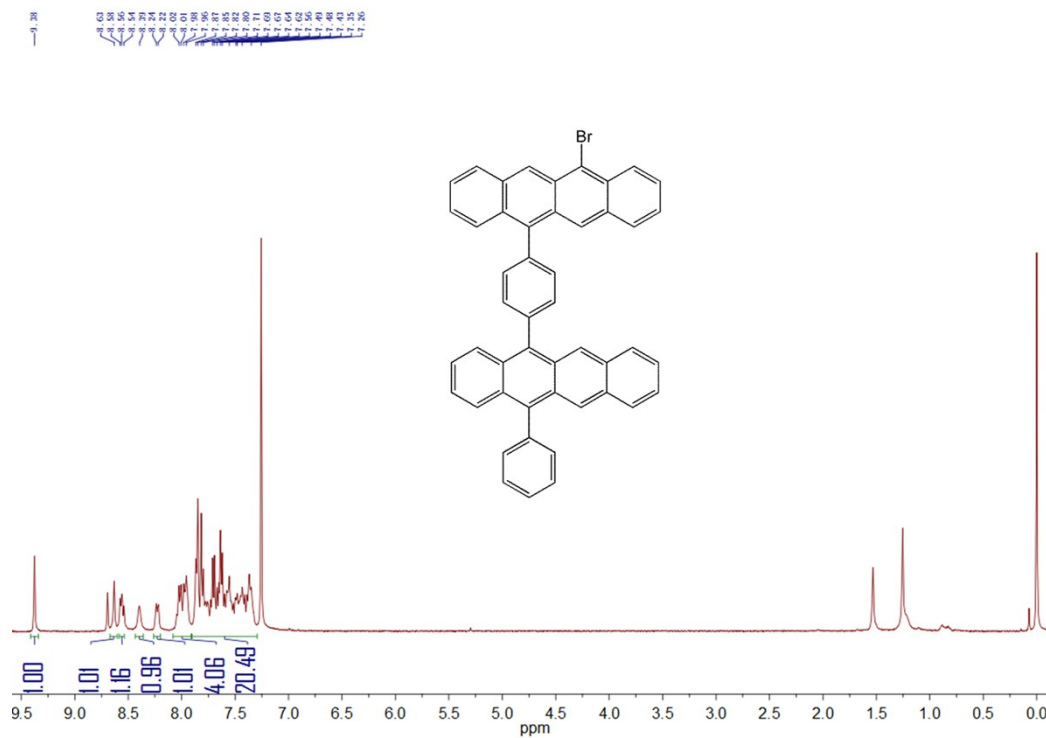


Fig. S14 The ^1H NMR spectrum of compound 10.

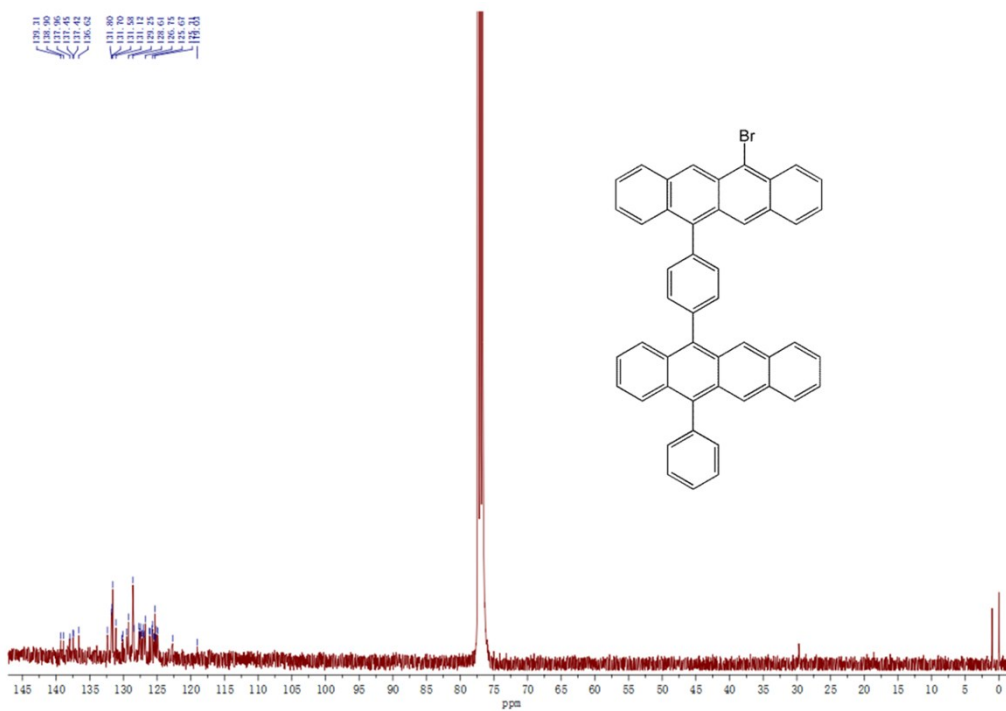


Fig. S15 The ^{13}C NMR spectrum of compound 10.

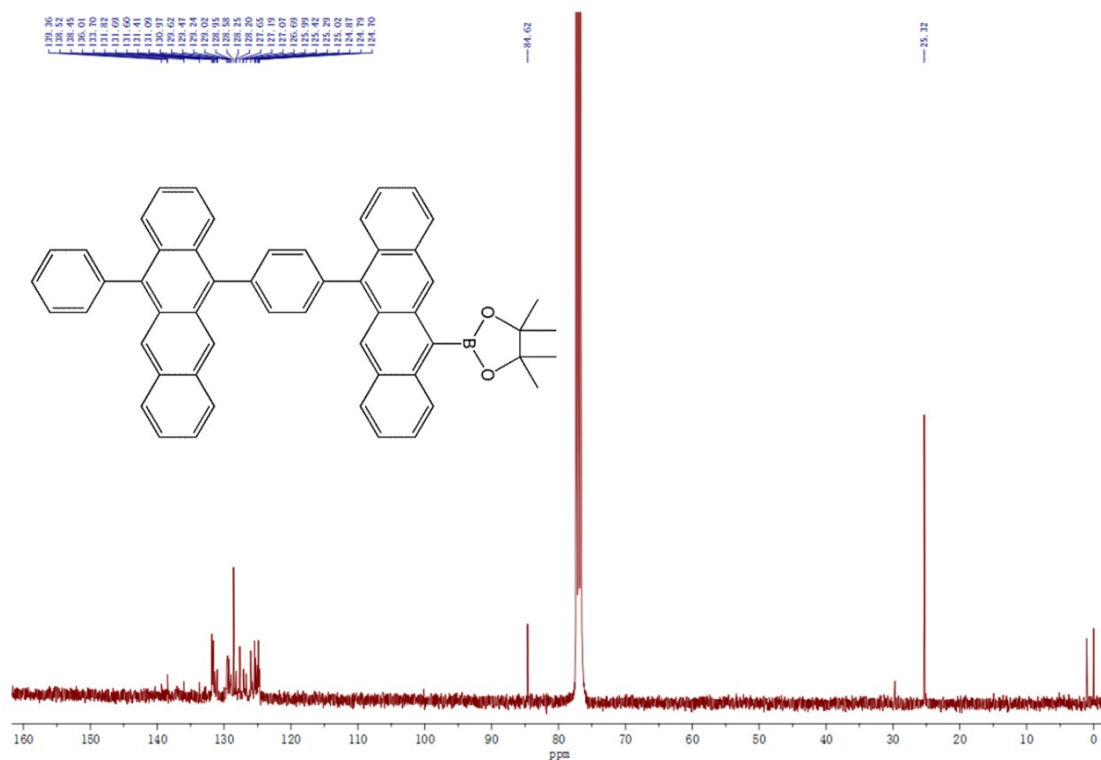


Fig. S18 The ¹³C NMR spectrum of compound 11.

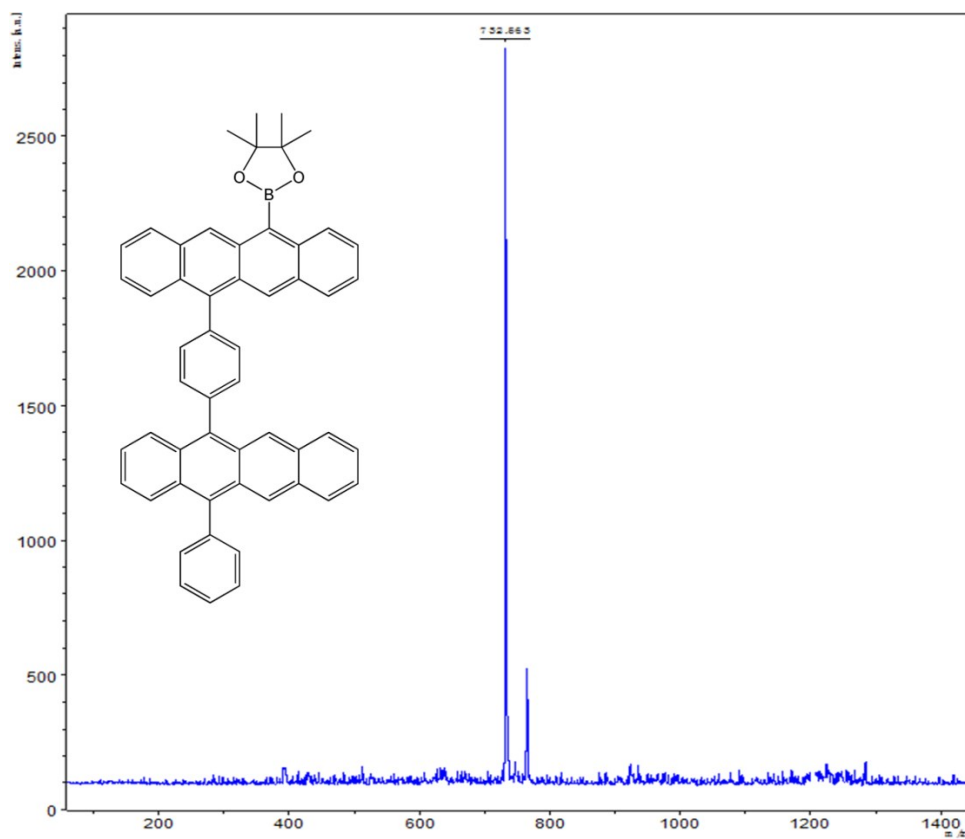


Fig. S19 The MALDI-TOF spectrum of compound 11.

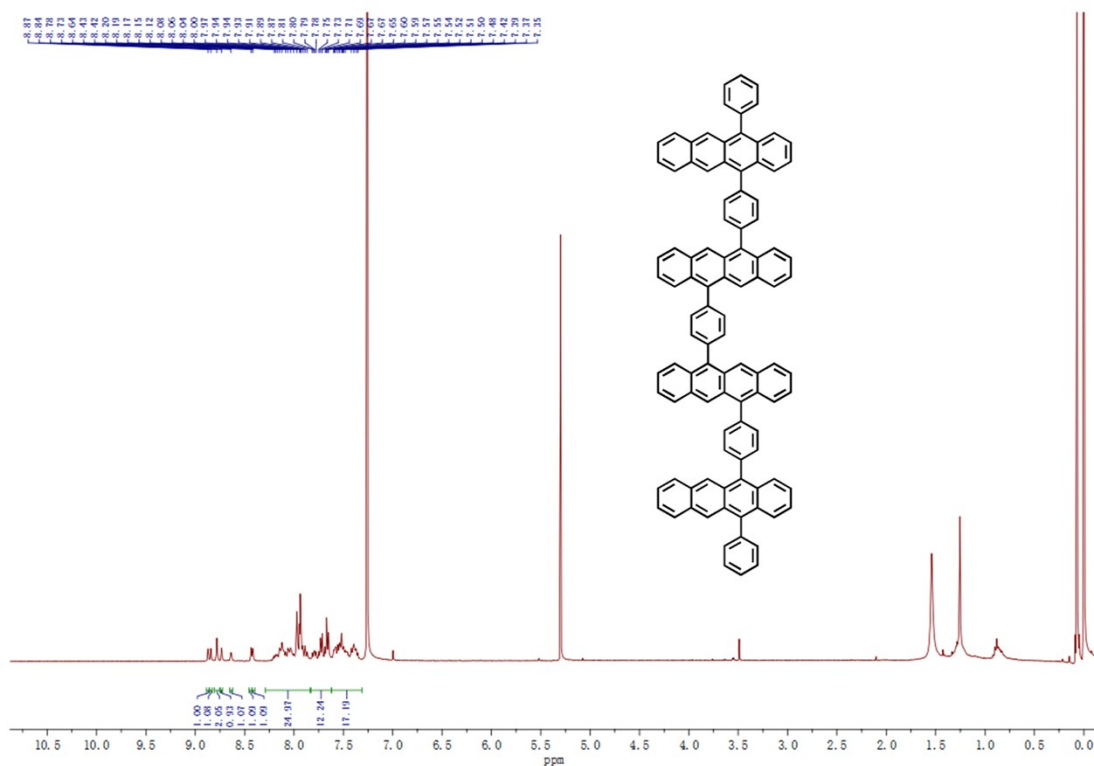


Fig. S20 The ¹H NMR spectrum of tetramer 4.

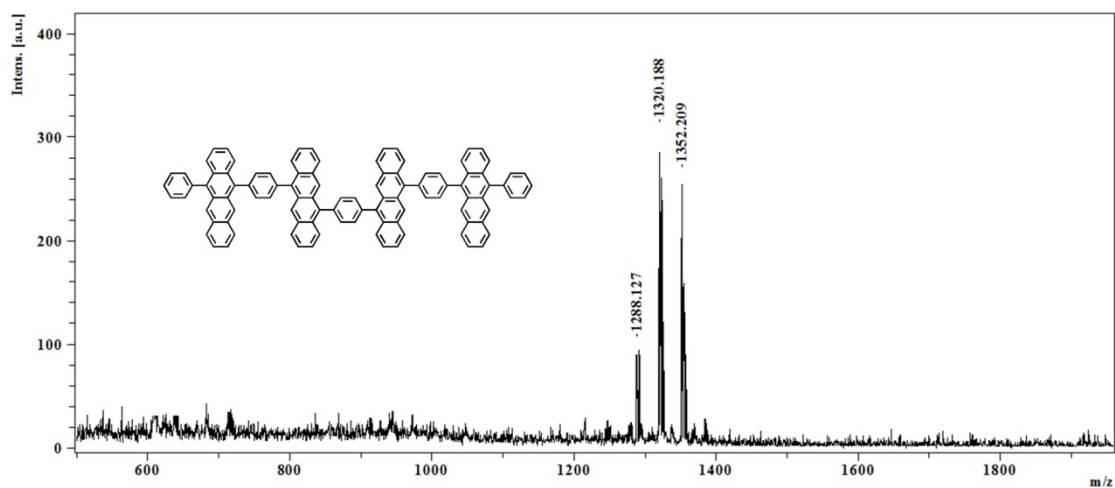


Fig. S21 The MALDI-TOF spectrum of tetramer 4.

Reference

1. H. Liu, R. Wang, L. Shen, Y. Xu, M. Xiao, C. Zhang and X. Li, *Org. Lett.*, 2017, **19**, 580-583.
2. P. C. Hariharan, J. A. Pople, *Theor. Chim. Acta*, 1973, **28**, 213-222.
3. M. M. Francl, W. J. Pietro, W. J. Hehre, J. S. Binkley, M. S. Gordon, D. J. DeFrees and J. A. Pople, *J. Chem. Phys.*, 1982, **77**, 3654-3665.
4. M. Frisch, G. Trucks, H. Schlegel, G. Scuseria, M. Robb, J. Cheeseman, G. Scalmani, V. Barone, B. Mennucci and G. Petersson, *Gaussian Inc., Wallingford, CT*, 2010.
5. S. T. Roberts, R. E. McAnally, J. N. Mastron, D. H. Webber, M. T. Whited, R. L. Brutchey, M. E. Thompson and S. E. Bradforth, *J. Am. Chem. Soc.*, 2012, **134**, 6388-6400.
6. S. N. Sanders, E. Kumarasamy, A. B. Pun, M. T. Trinh, B. Choi, J. Xia, E. J. Taffet, J. Z. Low, J. R. Miller, X. Roy, X. Y. Zhu, M. L. Steigerwald, M. Y. Sfeir and L. M. Campos, *J. Am. Chem. Soc.*, 2015, **137**, 8965-8972.